International Journal for Housing Science and Its Applications
Publish August 6, 2025. Volume 46, Issue 3 Pages 4697-4710

https://doi.org/10.70517/ijhsa463402

Research on the Architecture of Intelligent Electrical Control Platform Based on Distributed Domain Control and Wireless Sensor Networks

Jian Hu[1,*] and Qingpu Hu[1]
[1] Department of Electrical Engineering, Yellow River Conservancy Technical Institute, Kaifeng, Henan, 475004, China
Corresponding authors: (e-mail: hjyrcti@163.com).

Abstract In order to effectively enhance the control effect of the electrical control platform, this paper proposes an intelligent electrical control platform based on wireless sensor network, in which the main circuit, control circuit and wireless communication unit are designed. Then from the H∞ control principle of distributed wide-area control technology and loop-forming control technology, the H∞ loop-forming control scheme and structure of the electrical control platform are designed. In order to verify the effectiveness of the method proposed in this paper, the H∞ control strategy and the performance of the electrical control platform are verified and analyzed. The results show that compared with the traditional PSS, the H∞ controller can significantly enhance the control performance of the electrical control platform, reduce the amount of overshooting, and improve the speed of the system to stabilize. The speed of the H∞ control strategy can be lower than about 150rad/min can be sustained at a higher current output, the speed of 480rad/min out of the vibration zone, the speed of 1000rad/min motor blocking, through the distributed domain control scheme, the motor is controlled by the distributed domain control scheme. The control effect of the electrical control platform can be significantly enhanced and the efficiency of the electrical control platform can be better ensured by distributed domain control and wireless sensor network.

Index Terms electrical control platform, H∞ control principle, loop forming, distributed domain control

I. Introduction

Intelligent electrical control systems are widely used in the fields of industrial automation, building intelligence, urban infrastructure management and energy system optimization, integrating advanced control, monitoring and communication technologies to achieve efficient management of electrical equipment and energy flow [1]-[3]. Energy management is one of the most critical functions in the system, which is directly related to the efficiency of energy use and cost control [4], [5]. The main problem facing the current energy management of intelligent electrical control systems is that the degree of intelligence is not high enough, and there is still room for improvement in data processing, energy monitoring and predictive analysis [6], [7].

Internet of Things (IoT) technology provides an effective way to solve the above problems due to its high connectivity and intelligent characteristics [8]. IoT technology can connect and communicate with numerous sensor devices in real time, which makes it possible to collect, process and analyze a large amount of energy usage data, improves the efficiency of data collection and analysis, and enables the system to make a quick response based on real-time data, optimize energy management strategies, and achieve energy saving and efficient use [9]-[11]. Therefore, exploring the optimization and application of IoT technology in the energy management of intelligent electrical control systems can enhance the performance of intelligent electrical control systems in energy management, improve the efficiency of energy use, reduce energy costs, and have a positive effect on the development of the electrical industry [12]-[15].

In this paper, with the goal of improving the control effect of electrical control platform, the framework of intelligent electrical control platform based on wireless sensor network is proposed, and the responsive power main circuit, control circuit and wireless communication unit are designed. On this basis, the H∞ control principle is introduced to establish the H∞ loop forming control scheme and structure of the electrical control platform. For the practical application feasibility of the method in this paper, the H∞ control strategy and the relevant performance of the electrical control platform are simulated, in order to provide a reference for the optimization of the electrical control platform.

II. Intelligent Electrical Control Platform Architecture

The electrical control system consists of a numerical control, a servo drive system, a power supply system, and numerous sensors. The CNC system is responsible for analyzing and executing the machining program and precisely scheduling the operations of the machine. The servo drive system is responsible for the precise control of the machine's feed axes and spindle movements, and the power supply system provides a stable and reliable power supply to the CNC. Sensors are responsible for capturing relevant positioning, speed and temperature data during machine operation. These subsystems work together to carry out the machining mission of the CNC machine. With the support of existing technology, how to further enhance the intelligent control of the electrical control system is an important research direction to realize the intelligent transformation of the electrical control system.

II. A. Components of the electrical control platform

II. A. 1) Hardware Component Description

(1) The contactor is an automatic switching appliance used to frequently and remotely disconnect and connect AC and DC main circuits and large-capacity control circuits. Its control object is mainly electric motor, can also be used to control other electric heaters, welding machines, electric loads, capacitor banks and electric lighting.

(2) Relay is an automatic switching appliance that breaks or turns on the control circuit according to the change of non-electrical quantity (pressure, speed, temperature, time, etc.) or electrical quantity (current, voltage, etc.). Thermal relay is a protection appliance that cuts off the circuit through the principle of thermal effect of electric current. Motor in operation will often encounter overload conditions, but as long as the overload is not serious, the winding does not exceed the allowable temperature rise, this overload is allowed. But if the overload situation is serious, long time, it will accelerate the aging of motor insulation, or even burn the motor.

(3) The fuse is a short-circuit protection appliance in the electric power traction system and low-voltage power distribution system. When used, the circuit to be protected by the series of fuses, when the current flowing through the fuse than the specified value is large, the heat generated by itself can make the fuse fuse, so that the circuit is automatically cut off to achieve short-circuit protection.

(4) Button is manual and can be automatically reset a master electrical, its control is convenient, simple structure, widely used in low-voltage control circuit. According to the use and structure of the different buttons are divided into stop button, start button and composite button.

(5) The changeover switch has the advantages of multi-position, small size, multi-contact, convenient operation, flexible installation, reliable performance, etc. It is mostly used as the introduction switch of the power supply in the electrical control line, and plays the role of power supply isolation, and it can also be used as the control switch to control the infrequent stopping and starting of the small-capacity asynchronous motors.

(6) Three-phase asynchronous motor is a motor that is supplied with power by simultaneously connecting to a 380V three-phase AC power supply (with a phase difference of 120 degrees). Since the rotating magnetic fields of the stator and rotor of a three-phase asynchronous motor rotate at different speeds and in the same direction, there is a rate of rotation difference, so it is called a three-phase asynchronous motor.

II. A. 2) Electrical control platform framework

The advantages and disadvantages of the platform hardware scheme design directly affect the design of the system software program and the realization of the overall performance. The functional composition of the intelligent appliance control system is shown in Figure 1, and the system is mainly composed of a video monitoring circuit, a main system circuit, a system control circuit and a system measurement circuit.

(1) The main purpose of the video monitoring system is to monitor the operation status of the system and photograph the ground target of the test, through the video monitoring can real-time monitoring of the test operation platform operation process, to ensure the safety of the test process.

(2) The main circuit of the system consists of a driver and a drive motor. The drive includes four drives, including horizontal running servo drive, frequency converter, rotary running servo drive and stepping motor drive, and the drive motor includes four motors, including horizontal running permanent magnet synchronous motor, three-phase asynchronous motor, stepping motor and rotary running permanent magnet synchronous motor, which corresponds to the four degrees of freedom of operation, namely, horizontal, lifting, rotating, and pitching [16].

(3) The core of the system control circuit is a programmable logic controller (PLC). The position sensor is powered by a 24V switching power supply, and the detection signal can be sent directly to the PLC for position control. The touch screen is also powered by 24V switching power supply, the touch screen as a carrier of human-computer interaction interface can communicate with the PLC data, the touch screen can be programmed through the configuration programming software, which can real-time reflection of the system's various degrees of freedom operating state and operating parameters, and at the same time, can be motion control. PLC can be relay and indicator components such as analog outputs, so as to carry out effective control.

(4) The measurement circuit of the system consists of three parts: single-phase AC stabilized purified voltage, linear power supply and linear power supply junction box, whose main function is to provide stable and pure three-phase AC power supply and 0-36V stable and reliable DC voltage source for radar test.

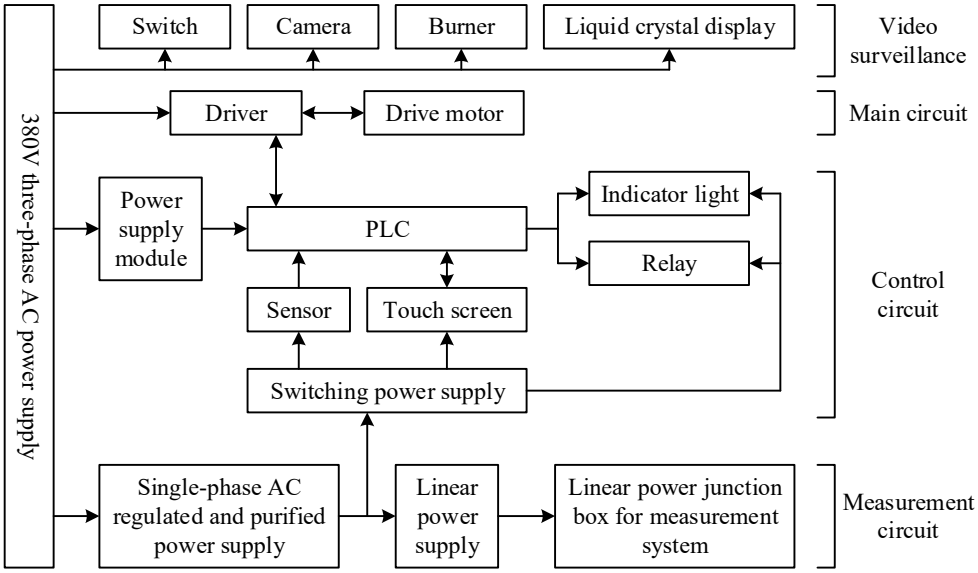

Figure 1: Hardware composition of the electrical control system

II. B.Electronic control system software design

II. B. 1) Electrical control system power main circuit design

The stepper motor used in this design is a two-phase hybrid stepper motor manufactured by S, model 103H7128, with a two-phase, eight-pole stator. Each phase winding has a center tap, so this motor is six-out. Its rated operating voltage is 15~220V, the highest phase current is 4A, and the DC power supply used in this design is 24V. Because this motor has a middle tap, six out of the line, different from the traditional eight out of the line two-phase motor, so its main circuit is also different from the traditional double-bridge structure.

Figure 2 shows the design framework of the power main circuit of the electronic control system. The two phase windings operate in a similar manner. The A-phase winding is used as an illustration, and the wiring of the A-phase winding is shown in Figure 2. The center tap is connected to the positive pole of the DC power supply, and the remaining two ends are connected to the negative pole of the power supply through switching tubes V1 and V2 and sampling resistor R1. The stepper motor operates with two directions of coil current, assuming that the direction of current in the A-phase coil is positive when switching tube V1 is closed and V2 is open, and the direction of current in the A-phase coil is negative when V1 is open and V2 is closed. From the working principle of the motor, it can be seen that a phase of the coil in a moment of the current direction can only be a direction, then the action of the switching tube V1 and V2 is complementary, when one is closed when the other must be open. VD1 and VD2 are the continuity diodes and R1 is the sampling resistor for phase A current.

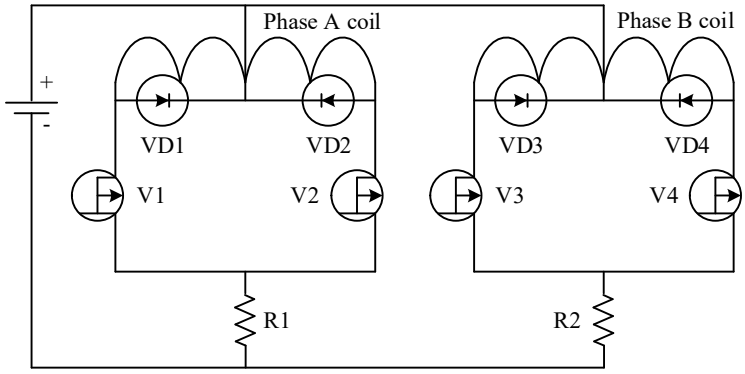

Figure 2: Design of the main power circuit of the electronic control system

The role of the sampling resistor is to sample the actual value of the current in the coil to be used as an input to the overcurrent protection circuit and the current feedback circuit. The premise of current sampling is that the resistor in the series does not affect the current of the original circuit, so the current sampling resistor should be small compared with the load resistance in the original circuit. In addition, because this resistor is strung into the main circuit, to flow through a large current, so it is necessary to choose a high-power, otherwise it will burn out or resistance value changes and can not work properly. And the signal after sampling will be used as the input of the overcurrent protection circuit and the current feedback circuit, so the resistance value of this resistor must be precise and not affected by the temperature change, so it is necessary to choose a precision resistor.

II. B. 2) Electronic control system control circuit design

The control circuit part is the operation carrier of the core control algorithm of the whole system, and it is the weak part of the whole system. The microprocessor outputs six PWM pulses through the corresponding control algorithms, which are used as the input signals of the inverter to control the output power of the inverter circuit and achieve the purpose of driving the stepping motor.

The microcontroller in this design is mainly used to realize the following functions: realizing the current loop vector control algorithm, realizing the spatial pulse width modulation algorithm (SVPWM), generating PWM pulses, sampling the feedback and processing the current signals, receiving the pulses, subdividing the current value, and the direction signals sent by the upper computer, and responding to various alarm signals such as overcurrent and overvoltage, as well as giving interrupt commands.

In order to meet the above requirements, in the microcontroller chip selection should pay attention to the following issues: the selected chip should be able to complete the complex data processing and control algorithms, real-time should be good; should have a large enough memory space. To have motor control required PWM output, AD sampling and other peripheral interfaces.

Based on the above analysis, and taking into account the cost, this system selects the ARM microcontroller STM32F103 as the core, STM32F103 uses a 32-bit RISC core Cortex-M3, which, compared with similar processors, possesses low power consumption, large flash memory space, high precision, comes with dead time control, and more peripheral interfaces.

II. B. 3) Electronic control system wireless communication unit design

(1) Wireless Sensor Network

Wireless sensor network is a network structure based on wireless communication technology, which consists of sensor nodes distributed in space, and realizes the monitoring and collection of field information through the collaborative work of sensor nodes.Sensor nodes in WSN are distributed in the monitoring area, and the sensor nodes can self-organize to form a network without human intervention. The nodes can be automatically configured and adjusted to each other according to the environment and network conditions to adapt to network topology changes and node failures. This distributed deployment makes the sensor network highly flexible and adaptable. Sensor nodes are usually powered by batteries, so energy consumption is an important consideration in WSNs. In order to extend the lifetime of the network, WSNs are usually designed with low power consumption, including low-power communication protocols, MAC protocols, network topology control, data processing and transmission mechanisms of the nodes.

Wireless sensors can be defined as a network of devices, denoted as nodes. Sensor nodes are divided into sensing nodes, routing nodes and aggregation nodes due to their different functions, and the mutual communication between nodes is realized through topology control. Since wireless sensor networks are constructed in a self-organizing manner, it is important to maintain network stability and anti-interference. Wireless sensor network topology can be divided into star topology, mesh topology and cluster topology.

(2) Wireless communication unit design based on wireless sensor network

In the intelligent electrical control platform established in this paper, the wireless communication module adopts CC2440 module that supports IEEE 802.15.4 protocol, and the design of the wireless communication unit mainly realizes the construction of the wireless transmission channel from the data acquisition node to the management node. It contains a total of eight wireless communication modules, respectively, as a wireless transmitter module and wireless receiver module, this part of the design is mainly to realize the 7RFD-1FFD star wireless personal area network networking, to realize the wireless radio frequency transmission of data. It is also connected with its front-end collection and processing unit and back-end host computer monitoring center to open up the data flow path from the terminal sensing node to the host computer management node.

The system uses IAR Embedded Workbench IDE integrated compilation and development environment for program design, Smart Flash Programmer to complete the program writing, debugging tools such as serial port debugging assistant. The design of the wireless communication unit mainly includes the wireless networking of the

system, the program design and implementation of the wireless receiving module and the wireless transmitting module.

III. Intelligent electrical control platform control design

In the intelligent electrical control system, it is more important to realize its intelligent control through microcontroller. Relying on the discrete automation execution mode of microcontroller, to assist in realizing the effective control of the electrical control system. With the continuous improvement of electronic technology, fully explore the application of microcontroller in the electrical control system has become an inevitable trend. Based on this, this paper establishes a loop forming controller based on H∞, in order to realize the efficient control optimization of intelligent electrical control system.

III. A. Distributed Wide Area Control Technology

III. A. 1) H∞ control principle

H∞ robust control theory combines the classical frequency-domain approach with the state-space method in modern cybernetics for multiple-input multiple-output (MIMO) systems, which designs closed-loop controllers by optimizing the infinite number of paradigms for certain performance metrics to achieve a good compromise between robustness and control performance [17]. The loop shaping design concept describes the design objective of the closed-loop system in terms of the open-loop transfer function, and by adjusting the open-loop transfer function of the system to satisfy the system performance requirements and stability boundaries in the low and high frequency bands, the closed-loop system can achieve the desired performance.

(1) H_∞-spaces and paradigms

A H_∞-space is a class of matrix function groups in which the functions are analytic and bounded in the open-loop right half-plane, and is a subspace of a L_∞-space (i.e., a Banach space). The RH_∞-infinite space is a real rational subspace of the H_∞-space, consisting of all regular, real rational transfer function matrices.

Univariate systems can be characterized by a Bird's graph, multivariate most systems are not suitable for Bird's graph representation and can be represented in singular value form. Since the transfer function matrix $G(j\omega)$ has the singular values $\sigma_1(\omega),\sigma_2(\omega),...,\sigma_m(\omega)$ are functions with ω as the independent variable whose frequency domain trajectories, called singular value curves, can be plotted. These singular value curves characterize the amplification of the system with respect to the input vector and are important indicators of robust control of multivariate systems [18].

The H_∞-paradigm is the paradigm of the transfer function matrix in the H_∞-space, defined as:

$$\| G \|_\infty = \sup_{\mathrm{Re}(s)>0} \bar{\sigma}[G(s)] \tag{1}$$

$$\sup_{\mathrm{Re}(s)>0} \bar{\sigma}[G(s)] = \sup_{\omega \in R} \bar{\sigma}[G(j\omega)] \tag{2}$$

where $\bar{\sigma}$ denotes the maximum singular value function. $\| G \|_\infty$ i.e., the upper definitive bound of the maximum singular value function of the transfer function matrix, whose actual physical meaning is the maximum magnitude of the response of all sinusoidal signals applied to the system, while any other signals can be synthesized from sinusoidal signals.

(2) Left Mutual Mass Decomposition

Two transfer functions $m(s),n(s)$ in RH_∞ are said to be $m(s),n(s)$ mutually prime if there exists $x(s),y(s) \in RH_\infty$ such that the equation $xm+yn=1$ holds.

The normalized left mutual prime decomposition is easily constructed by means of a state space approach. Let (A,B,C,D) be a minimal state-space realization of the transfer function matrix G, and the normalized left mutual prime decomposition $(\tilde{N},\tilde{M})$ of G can be defined by the following state-space realization:

$$\left[\tilde{N},\tilde{M}\right] \square \begin{bmatrix} A+HC & B+HD & H \\ R^{-1/2}C & R^{-1/2}D & R^{-1/2} \end{bmatrix} \tag{3}$$

where $H \square -(YC^H+BD^H)R^{-1}, R \square I+DD^H, S \square I+D^HD$, Y are the unique positive definite solutions of the following generalized filtered algebraic Raccati equations, viz:

$$(A-BS^{-1}D^{H}C)Y+Y(A-BS^{-1}D^{H}C)^{H}-YC^{H}R^{-1}CY+BS^{-1}B^{H}=0 \tag{4}$$

(3) Uncertainty modeling. In the process of mathematically modeling the controlled object for controller design, in order to balance model simplicity and accuracy, the nominal model used for controller design is not the same as the actual controlled object, and the difference between the actual object and the nominal model is called modeling error. Modeling error may appear in many ways, for example, most systems usually use linear nominal models in the design process, while the actual physical system always exists a certain nonlinearity, since the linear model can not represent the nonlinear behavior, so modeling error must be introduced. Another source of modeling error is the error caused by imprecise model parameters, which is particularly common when using system identification to obtain nominal models. Uncertainty is categorized as “structured” or “unstructured”. Unstructured uncertainty is uncertainty for which there is no information about the mechanism of action other than an upper limit on its magnitude (i.e., frequency magnitude or singularity), while structured uncertainty is uncertainty for which “structural” information is available. Uncertainty that provides structured information is not common, so we mainly consider unstructured uncertainty.

III. A. 2) Loop Forming Control Principle

The basic structure of the H∞ loop shaping control is shown in Fig. 3, which synthesizes classical control and modern robust optimization control in a single framework, giving the electrical control platform excellent performance for dynamic tracking of input signals and decoupling of channels [19].

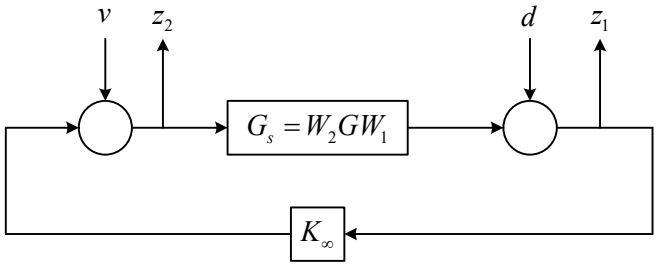

Figure 3: H∞ The basic structure of loop forming control

The G-array in the figure is the time-invariant model of the incremental linearized dynamics of the controlled object in a certain operating state. The weighted diagonal arrays w_1 and w_2 are set to shape the open-loop singular values of the G-array (which are equivalent to the scalar system control object amplitude-frequency characteristics). The open-loop transfer function array shaped by the weighted configuration is G_s and:

$$G_s=W_2GW_1 \tag{5}$$

The weighted array W_2 in the feedback channel contains a low-pass filter to suppress the sensor noise and an overshooting lag corrector to improve the robustness, and the weighted array W_1 in the forward channel is in the form of a proportional+integral (P+I), where the integral link is used to increase the low-frequency gain in order to improve the steady-state tracking accuracy of the present channel.

After the loop is shaped according to the above design ideas, then H_∞ should be designed. Controller $K_\infty(s)$ array. The control array $K_\infty(s)$ should be introduced in such a way that the inverse of the $[d,v]^T$ to the error $[z_1,z_2]^T$ of the transfer function array maximizes the inverse of the H_∞ paradigm. Namely:

$$\max_{stabK_\infty}\left\|\begin{bmatrix}d\\v\end{bmatrix}\rightarrow\begin{bmatrix}z_1\\z_2\end{bmatrix}\right\|^{-1}=\varepsilon \tag{6}$$

where d is the perturbation input, v is the control input, z_1 is the output under the perturbation input, and z_2 is the output error under the control input. $\in$ can characterize the stability margin of the system. $\in$ should be chosen in [0,1] to represent the robustness to be achieved by the system. By experience $\in$ greater than 0.3 is preferred. For a single-input single-output system, the value of $\in$ can correspond to a certain magnitude margin and phase angle margin. It can be shown that the amplitude-phase margin of a single loop is related to $\in$. where

the magnitude valley $Gm = \pm 20\log_{10}\frac{1+\in}{1-\in}$ and the phase angle margin $Pm = 2\arcsin\in$. Thus $\in$ = 0.35 corresponds to an amplitude margin of ±6.3 dB and a phase angle margin of 40.9deg.

The physical significance of Eq. (6) as a performance metric for the design of the H_w loop-forming controller is quite obvious. Because the infinite parameter of a certain function $f(s)$ is defined as:

$$\| f(s) \|_\infty = \sum_{s=0}^{\infty} | f(s) | \tag{7}$$

So for a scalar system, $\| f(s) \|_\infty$ corresponds to the sum of the magnitudes of all the amplitude-frequency characteristics of the function $\omega = 0$ to ∞.

III. B. Electronic control platform controller design

III. B. 1) H_∞ loop shaping control scheme

In the intelligent electrical control platform, the main and control circuits are linearized and their mathematical models are organized in the form of radial nonlinear systems, viz:

$$\begin{cases} \dfrac{dx}{dt} = f(x) + g_1(x)u_1 + g_2(x)u_2 \\ y_1 = h_1(x) \\ y_2 = h_2(x) \end{cases} \tag{8}$$

where $f(x), g(x)$ and $h(x)$ are vector fields. The mathematical model of the rotor-side converter is compared with the standard affine nonlinear system model for the selection of relevant parameters. The selection of vector fields f and g is determined by the sufficient condition of the Li derivative, and the selection results are as follows:

$$f = \begin{bmatrix} -\dfrac{R_r}{\sigma L_r} i_{rd} + \omega_1 i_{rq} - \omega_r i_{rq} \\ -\dfrac{R_r}{\sigma L_r} i_{rq} - \omega_1 i_{rd} + \omega_r i_{rd} \end{bmatrix} = \begin{bmatrix} f_1 \\ f_2 \end{bmatrix} \tag{9}$$

$$g = \begin{bmatrix} \dfrac{1}{\sigma L_r} & 0 \\ 0 & \dfrac{1}{\sigma L_r} \end{bmatrix} = \begin{bmatrix} g_1 & g_2 \end{bmatrix} \tag{10}$$

This is then combined with the LMI algorithm to convert it to a linear system form, i.e:

$$\begin{cases} \dot{P}_s = v_{r1} \\ \dot{Q}_s = v_{r2} \end{cases} \tag{11}$$

$$\begin{cases} v_{r1} = \dfrac{L_m u_{sd}}{\sigma L_r L_s}(R_r i_{rd} - \sigma L_r(\omega_1 - \omega_r) i_{rq} - u_{rd}) \\ v_{r2} = \dfrac{L_m u_{sd}}{\sigma L_r L_s}(-R_r i_{rq} - \sigma L_r(\omega_1 - \omega_r) i_{rd} + u_{rq}) \end{cases} \tag{12}$$

The transformation of Eq. (12) leads to the feedback linearized controller for the rotor side converter as follows:

$$\begin{cases} u_{rd} = -\dfrac{\sigma L_r L_s}{L_m u_{sd}} v_{r1} + R_r i_{rd} - \sigma L_r(\omega_1 - \omega_r) i_{rq} \\ u_{rq} = \dfrac{\sigma L_r L_s}{L_m u_{sd}} v_{r2} + R_r i_{rq} + \sigma L_r(\omega_1 - \omega_r) i_{rd} \end{cases} \tag{13}$$

In the right-hand side variables of Eq. (13), all of them are available except the control inputs v_{r1} and v_{r2} which are not available. The values of v_{r1} and v_{r2} can be given by designing a linear controller by Eq. (11), and the above equation can be obtained by Laplace transform:

$$\begin{cases} P_s(s) = V_{r1}(s)/s \\ Q_s(s) = V_{r2}(s)/s \end{cases} \tag{14}$$

From Eq. both have the same transfer function $1/s$, i.e., $G_{r1}(s) = G_{r2}(s) = 1/s$, and letting P_s^* and Q_i^* be the reference values of the variables, V_{r1} and V_{r2} can be expressed as:

$$\begin{cases} V_{r1}(s) = C_{r1}(s)(P_s^*(s) - P_s(s)) \\ V_{r2}(s) = C_{r2}(s)(Q_s^*(s) - Q_s(s)) \end{cases} \tag{15}$$

where C_{r1}, C_{r2} denotes the linear controller of the rotor side converter.

From Eq. (14), the two controlled objects of the linear controller of the rotor-side converter are $G_{r1}(s) = G_{r2}(s) = 1/s$, so both of them can be used the same linear controller structure, set $G_{r1}(s) = G_{r2}(s) = 1/s = G(s)$, and it is easy to derive the transfer function for the rotor-side converter. The transfer function of the closed-loop system is:

$$T_i(s) = \frac{G(s)C_n(s)}{1 + G(s)C_n(s)}, i = 1,2 \tag{16}$$

where C_n denotes the linear controller of the rotor-side converter.

The control error transfer function is:

$$S_i(s) = 1 - T_i(s) = \frac{1}{1 + G(s)C_n(s)}, i = 1,2 \tag{17}$$

Since the rotor-side converter is transformed into two single-input single-output linear control systems in this paper, the closed-loop system transfer function can be used as the complementary sensitivity function and the control error transfer function as the sensitivity function.

When the system is stabilized, the frequency response of $\delta_i(s)$ and $T_i(s)$ need to be satisfied by the small gain theorem:

$$|\delta,(j\omega)||T_t(j\omega)| < 1 \tag{18}$$

is obtained by transforming the above equation:

$$|\delta_i(j\omega)| < 1/|T_i(j\omega)|_\infty \tag{19}$$

where $\|\cdot\|_\infty$ denotes the H∞ paradigm of the transfer function, which behaves as the maximum magnitude of the frequency response when the transfer function is stable.

From Eq. (19), $|T_i(j\omega)|$. is inversely proportional to $|\delta_i(j\omega)|$, when $|T_i(j\omega)|$. The smaller it is, the greater perturbation $|\delta_i(j\omega)|$ it can withstand, so $M_i = 1/|T_i(j\omega)|_\infty$ is taken as the stability margin for the controller design.

In order to facilitate subsequent controller calculations and the fact that the nonstructural perturbation $\delta_i(j\omega)$ usually increases with frequency, a high-pass filter $W_{\delta_i}(s)$ can be used as a substitute for $\delta_i(s)$ in Eq. (19), i.e.:

$$|W_{\delta i}(j\omega)||T_i(j\omega)| < 1 \tag{20}$$

For the above equation, it is necessary to test whether the conditions can be satisfied in the range of $\omega \in (-\infty, \infty)$. In order to simplify the calculation process, the above equation can be transformed into the H∞ paradigm form. That is:

$$\|W_{si}(j\omega)T_i(j\omega)\|_{si} < 1 \tag{21}$$

When the controller design conforms to the above equation, it is able to make $|W_\alpha(j\omega)||T_i(j\omega)|<1$, which further transforms to $|T_i(j\omega)|<1/|W_n(j\omega)|$ to satisfy that $T_i(s)$ has a low-pass frequency response, realizing a high tolerance to the usually large unstructured model perturbations $\delta_i(s)$. Therefore, the above equation enables controller design to ensure that the closed-loop system remains stable in the presence of perturbations.

From the above equation, it can be seen that when the system's ability to resist parameter uncertainty is stronger, the smaller $|p_i(j\omega)|$ is, however, due to $T_i(j\omega)+S_i(j\omega)\equiv 1$, then it will lead to a larger control error, and there is a contradiction in the parameter selection between the two. Therefore, the controller design about the sensitivity function $S_i(j\omega)$ is weighted by the frequency-dependent performance $W_{pi}(j\omega)$ such that:

$$\|W_\mu(j\omega)S_i(j\omega)\|_\omega<1 \tag{22}$$

Since the control error arises against the control inputs and the inputs to the control are usually low-frequency, the controller is designed for the above equation using a low-pass pooled waveform $W_{pl}(j\omega)$. When the controller design conforms to the above equation, it is able to make $|W_n(j\omega)||S_i(j\omega)|<1$, which is further transformed to $|S_i(j\omega)|<1/|W_n(j\omega)|$ to satisfy the $S_i(s)$ has a high-pass frequency response and is realized to have a small control error for inputs that are typically low-frequency.

III. B. 2) H∞ loop forming control structure

Based on the H∞ control theory and loop forming control principle, combined with the H∞ loop forming control scheme given in Section 3.2.1, the design flow of the H∞ loop forming controller of the intelligent electrical control platform is obtained as shown in Figure 4.

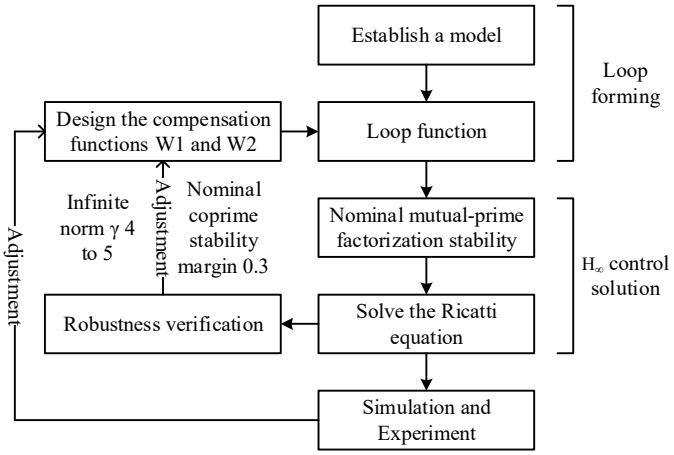

Figure 4: H∞ The design process of loop forming control

Step1 First, the controlled object is modeled and loop shaped by the front-back compensation function. The controlled object is made to be the desired shape, and the front-back compensation function cannot contain zero poles that make the controlled object unstable.

Step2 Decompose the resulting system into nominal mutual quality factors and transform it into an optimal H∞ solution problem, solving the Riccati equation to obtain the H∞ loop forming controller of the system.

Step3 Perform robustness calibration on the resulting closed-loop system to ensure the robustness of the system. If the resulting infinite parameter and the nominal mutual quality factor stability margin do not meet the design requirements, then return to Step1 to redesign the system before and after the compensation function.

Step4 Continue to adjust the front and back compensation functions in simulation and experiment, so that the resulting H∞ loop forming controller achieves the optimal control effect.

The design of the controller and the verification of the simulation are done in MATLAB/Simulink. According to the distribution of the system's zero poles, and considering the model of the system, the requirements of robustness, and adjusted according to the simulation for many times, the compensation function is selected to loop-form the system. The right plane unstable zeros in the system are guarded by a left half-plane pole, which will attenuate the gain of the unstable zeros to a constant value over the full frequency band, but this will also cause the phase margin

of the system to attenuate to a greater extent, but as long as the cutoff frequency of the system is sufficiently advanced, the system is still stable. The compensation functions W_1 and W_2 selected are expressed as:

$$\begin{cases} W_1 = k\dfrac{(500/s+0.08)}{(s+1.5625\times10^4)} \\ W_2 = I \end{cases} \tag{23}$$

where k is the gain, which can be adjusted, by changing k will not change the effect of zero-pole compensation, but can change the dynamic response speed and robustness of the system.

If higher order loop shaping design can be carried out, better control effect can be achieved, but it should be considered that the order of the controller should not be too high.

IV. Intelligent appliance control platform simulation analysis

The electrical control platform utilizes the basic technology and knowledge of several subject areas, such as electrical automation, computer discipline, PLC frequency control, etc., which is a comprehensive and practical system. It has changed from the traditional single device control to a control strategy based on electrical control, which internally contains relays, contactor hardware wiring, etc., and has changed the defects of the single function of the fixed platform. This chapter focuses on examining the performance of the H∞ loop forming control strategy and the electrical control platform given in the previous section as a way to promote innovative changes in the electrical control platform.

IV. A. Validation of the effectiveness of the H∞ control strategy

IV. A. 1) Mechanical power small disturbance control effect

In order to verify the control effect of the electrical control strategy designed in this paper based on the H∞ loop forming principle on the electrical control platform, this paper establishes a nonlinear model of the test system in MATLAB and carries out linearization analysis at different control points. Based on the weighting function matrix selection method given in the previous section, a suitable weighting function matrix is selected for loop forming of the controlled object before the H∞ controller design of the test system.

The linear H∞ controller without considering the saturation effect and the controlled object will form a closed-loop system. In this paper, the electrical control platform will be simulated and verified in the case of small perturbations in mechanical power. The details are as follows:

At t=2s, it is assumed that the mechanical power output from the prime mover of the generator undergoes a small perturbation and the output is increased by 100, at this time, since the perturbation is a small perturbation, the system in question is the static stability of the system under the action of the controller. The traditional PSS, the traditional H∞ controller and the H∞ controller of this paper are selected as a comparison, and the variation curves of the electrical control platform under the action of different controllers are obtained as shown in Fig. 5. Among them, Fig. 5(a)~(b) shows the simulation curves of rotational speed difference and line delivered power of G_{r1}, G_{r2} respectively.

It can be seen from the simulation diagram that when the output power of the prime mover changes, the relevant parameters of the generator and the various quantities of the system have a great impact, and under the action of each controller, they can finally be stabilized near the stable value, and it can be seen that the robust H∞ controller can improve the control performance and reduce the overshoot compared with the traditional PSS, so that the system tends to be stable faster. Compared with the traditional method, the H∞ controller designed by the selected weight function method has a smaller overshoot, which can more effectively suppress the low-frequency oscillation in the interval and better ensure the static stability of the electrical control platform.

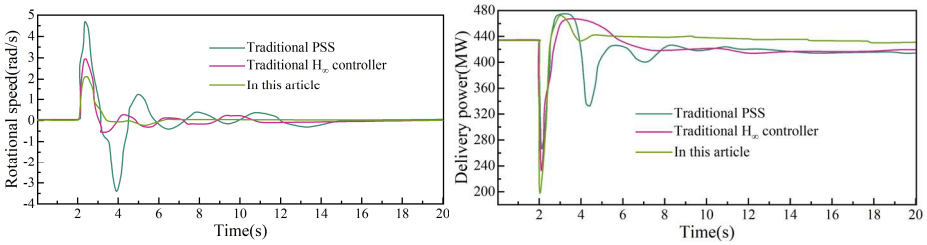

(a) G_{r1}, G_{r2} the rotational speed difference (b) Transmission power of line

Figure 5: There is a small disturbance in the mechanical power

IV. A. 2) DC Load and Filter Inductor Uptake

Under the H∞ controller, this paper further explores the control effect on the electrical control platform under the DC load mutation and filter inductance parameter ingestion, and analyzes it through simulation. The simulation results are shown in Fig. 6, where Figs. 6(a)~(b) show the simulation curves of DC load mutation and filter inductor ingestion, respectively.

(1) DC load mutation. The electrical control platform is lightly loaded at the initial moment, and the DC load power is set to change abruptly from 4kW to 10kW (load disturbance of 150%) at 2s, and the simulation ends at 20s. The DC voltage fluctuation of the DC bus is basically the same, and the DC voltage of the DC bus is used as an observation object to analyze and compare the stability of the DC voltage before and after adding the robust controller. As can be seen from Fig. 6(a), the DC voltage oscillation disperses when the DC load power suddenly increases to 10 kW in 2 s. This is due to the insufficient robustness of the power-voltage sag control, which results in the system not being able to maintain stable operation under load disturbances. When selecting the front and rear weight functions based on the H∞ loop shaping method, the low-frequency disturbance suppression capability of the system and the signal tracking performance are fully considered, so the designed robust controller can effectively suppress the low-frequency oscillation of the system when the load power is increased suddenly and make the system reach a new stable state quickly.

(2) Filter inductor parameter ingestion. Set both ends of the source-side filter inductance parameters change from 2.0mH to 2.40mH at 0s, and the simulation ends at 20s. The DC voltage fluctuation of the DC bus is basically the same, and the DC voltage of the DC bus is taken as the observation object to analyze and compare the stability of the DC voltage before and after adding the robust controller. From Fig. 6(b), it can be seen that the DC bus voltage oscillation is destabilized based on the power-voltage droop control when the 0s system filter inductor parameter ingress occurs, which is due to the fact that the power-voltage droop control is based on the system's accurate linear model for the design of the controller without considering the system parameter ingress caused by internal and external factors, and the robustness is insufficient. In this paper, the robust stabilization controller based on the H∞ loop shaping method is designed based on the nominal model and takes into account the uncertainty of the mutual quality factor of the system, so that it is insensitive to the filtering inductor parameter uptake, and still maintains the stability of the system dc bus voltage.

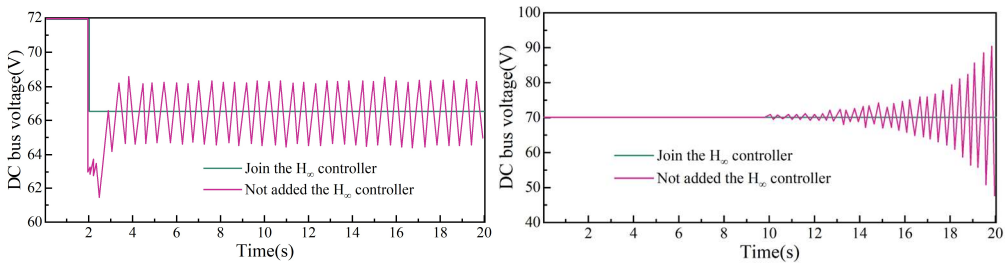

(a) Sudden change of DC load (b) Filter inductor perturbation

Figure 6: Control simulation of H∞ controller

IV. B. Electrical control platform performance verification

IV. B. 1) Control effect of the motor output matrix

Output torque is one of the important parameters for evaluating stepping motors, and it is also an index reflecting the motor's ability to carry load. Because the output torque of a two-phase stepping motor is proportional to its phase current, and the output torque of the motor cannot be measured directly in the experimental conditions, the experimental purpose is achieved by measuring the phase current of the motor. The electrical control platforms under the traditional PI and PD control strategies are selected as a comparison, and the results of the motor output torque under three different electrical control platforms are obtained as shown in Fig. 7. Among them, Fig. 7(a)~(c) shows the simulation results under PI, PD and H∞ control strategies, respectively.

When the electrical control platform in the PI control strategy, its speed in the lower than 240rad/min or so can continue to maintain a higher current output, with the speed of the torque into the attenuation of the state, the current drops sharply and vibration in the speed of 630rad/min or so, and then the speed of the motor blocked at 800rad/min or so. It can be seen that the electrical control platform in the current loop controller using a separate PI control when the speed in the 0-240rad/min response speed, the output holding torque to maintain a long time, but the speed of 800rad/min or more when the output torque decreases to lead to the load can not be brought to cause blocking.

When the electrical control platform in the PD control strategy, its speed in the lower than 400rad/min or so when the current continues to decline, in the speed of 400rad/min or so into the vibration, in the speed of 550rad/min or so out of the vibration zone, the speed of the motor blocking in the 1000rad/min or so blocked, than the blocking of the speed of the PD control to improve 25%. It can be seen that the electrical control platform uses a separate PD control in the current loop controller, and the current continues to decay when the speed is 0-400 rad/min, while the output torque of the two-phase stepper motor continues to drive the load when the speed is 500-1000 rad/min.

The use of H_∞ control strategy in the electrical control platform, the speed in the lower than 150rad/min or so can also continue to maintain a higher current output, and the use of PI control alone when the speed of 0-240rad/min, the same situation, to maintain the PI control continues to maintain the torque output, in the rotational speed of 320rad/min or so, into the vibration, in the speed of 480rad/min or so out of the vibration zone. /min or so out of the vibration zone, the speed of 1000rad/min motor blocking, retaining the PD control when the speed of 600-1000rad/min motor output torque can continue to drive the load running.

In summary, the use of this paper's H_∞ controller designed based on the H_∞ loop forming principle in the electrical control platform can significantly maintain the motor output torque of the electrical control platform and provide support for the high efficiency of the electrical control.

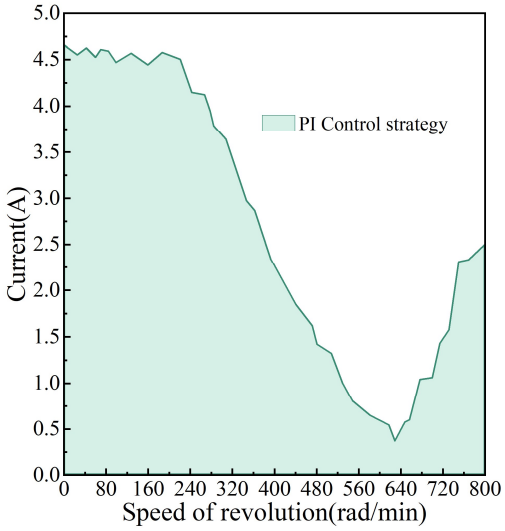

(a) PI Control strategy

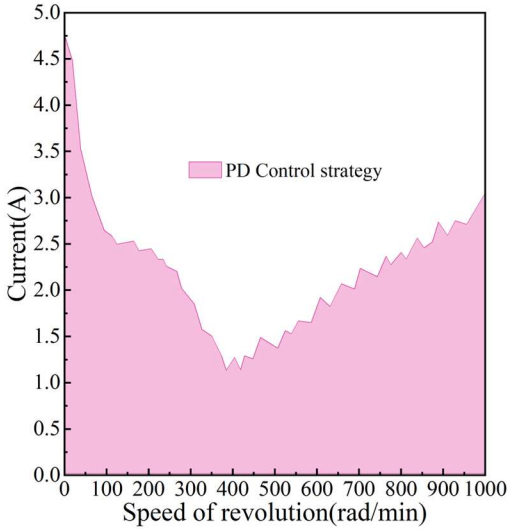

(b) PD Control strategy

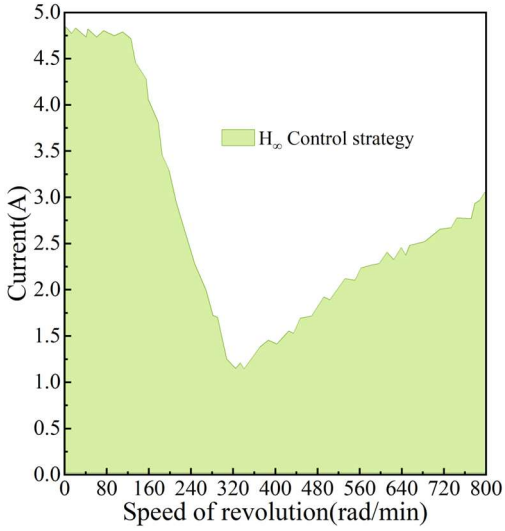

(c) H_∞ Control strategy

Figure 7: Output torque of the motor

IV. B. 2) No-load position control of electrical machinery

In order to verify the effectiveness of the H∞ controller designed in the previous paper, the algorithm is verified on the closed-loop control simulation system and experimental platform built. Test conditions for the 24V excitation voltage, the motor for the no-load condition, the control strategy are used H∞ control, tracking position instructions are positive and negative 500 pulse square wave, the simulation model of the motor parameters used in the simulation model has been measured experimental parameters, so that it has a comparable with the actual motor. The position controllers use H∞ controller and traditional PID controller respectively, and the simulation results are shown in Fig. 8. Figure 8(a)~(b) are the comparison results before and after optimization, respectively.

From the above simulation, it can be seen that in the case of no load motor, the electrical control platform using PID control and H∞ control can achieve better steady state accuracy, but the two control algorithms in the dynamic performance of the slight difference in Figure 8(a) simulation results in the two algorithms of the rise time is the same, but the position response of the PID control under the overshooting exists, which can be adjusted by adjusting the proportionality constants of the outer loop of the position or the differential constant to improve it. Figure 8(b) is the simulation waveform after the optimization of the outer loop parameters under PID control, and it can be seen that the difference between the two control algorithms at this time is not significant, and both have a faster response speed and no overshooting. The simulation results do not directly illustrate the advantages and disadvantages of PID control and H∞ control, but in terms of the difficulty of debugging the controller, PID control using the position loop and the two current inner loop composition, the position loop if the use of PD control and the use of current inner loop PI control, then the use of PID control needs to be set to more than one control parameter, while the H∞ control only needs to be set to two. In addition, PID control is not designed based on stability, when the parameter design is not reasonable, it is very easy to respond to overshooting, oscillation and so on, while for H∞ control, the system stability is generally guaranteed, and thus in the parameter debugging of the H∞ control than the PID control and some simple. In summary, the introduction of H∞ controller in the electrical control platform, can significantly enhance the control performance of the electrical control platform, and the overall debugging difficulty is lower, can be better applied to the actual electrical control.

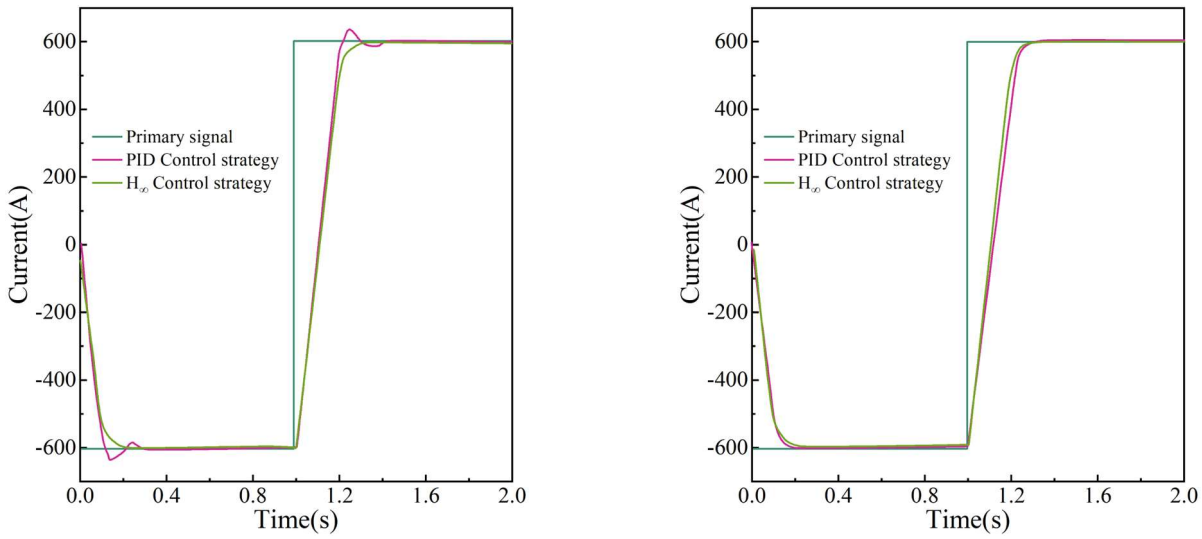

(a) before optimize (b) After optimize

Figure 8: Airborne simulation waveform

V. Conclusion

The article proposes an intelligent electrical control platform architecture, introduces the distributed wide-area control technology H∞ loop forming control principle to design the controller of the electrical control platform, and verifies the specific performance of the controller and the electrical control platform through simulation analysis. The results show that the robust H∞ controller can improve the control performance and reduce the amount of overshooting compared with the traditional PSS, which makes the system stabilize faster. The robust stabilization controller is insensitive to the filter inductor parameter ingress, which can effectively ensure the stability of the system DC bus voltage.

In addition, using the H∞ control strategy, the rotational speed can continuously maintain a higher current output when it is lower than about 150 rad/min, enter the vibration when the rotational speed is about 320 rad/min, come

out of the vibration zone when the rotational speed is about 480 rad/min, and the motor is blocked when the rotational speed is at 1,000 rad/min, which retains the output torque of the motor to continuously drive the load to run.

Therefore, the intelligent electrical control platform combined with distributed domain control can ensure efficient control efficiency, as well as effectively ensure the smoothness of the motor output matrix and bus voltage.

References

[1] Zhang, L. M., Liu, B. C., Tang, Q. H., & Wu, L. P. (2014, September). The development and technological research of intelligent electrical building. In 2014 China International Conference on Electricity Distribution (CICED) (pp. 88-92). IEEE.

[2] Kryukov, O. V. (2013). Intelligent electric drives with IT algorithms. Automation and Remote Control, 74(6), 1043-1048.

[3] Zeynal, H., Eidiani, M., & Yazdanpanah, D. (2013, January). Intelligent control systems for futuristic smart grid initiatives in electric utilities. In Conference Paper January (pp. 315-319).

[4] Logenthiran, T., Naayagi, R. T., Woo, W. L., Phan, V. T., & Abidi, K. (2015). Intelligent control system for microgrids using multiagent system. IEEE Journal of Emerging and Selected Topics in Power Electronics, 3(4), 1036-1045.

[5] Kaymanesh, A., Babaie, M., Chandra, A., & Al-Haddad, K. (2021). PEC inverter for intelligent electric spring applications using ANN-based controller. IEEE Journal of Emerging and Selected Topics in Industrial Electronics, 3(3), 704-714.

[6] Nie, G., & Xu, Y. (2021, April). Research on the application of intelligent technology in low voltage electric automation control system. In Journal of Physics: Conference Series (Vol. 1865, No. 2, p. 022072). IOP Publishing.

[7] Hou, S., Chu, Y., & Fei, J. (2021). Robust intelligent control for a class of power-electronic converters using neuro-fuzzy learning mechanism. IEEE Transactions on Power Electronics, 36(8), 9441-9452.

[8] Kaleybar, H. J., Kojabadi, H. M., Fazel, S. S., & Foiadelli, F. (2018). An intelligent control method for capacity reduction of power flow controller in electrical railway grids. Electric Power Systems Research, 165, 157-166.

[9] Feng, H. (2018, September). The application of artificial intelligence in electrical automation control. In Journal of Physics: Conference Series (Vol. 1087, No. 6, p. 062008). IOP Publishing.

[10] Bedi, G., Venayagamoorthy, G. K., Singh, R., Brooks, R. R., & Wang, K. C. (2018). Review of Internet of Things (IoT) in electric power and energy systems. IEEE Internet of Things Journal, 5(2), 847-870.

[11] Hassan, J. A., & Jasim, B. H. (2021). Design and implementation of internet of things-based electrical monitoring system. Bulletin of Electrical Engineering and Informatics, 10(6), 3052-3063.

[12] Chen, Z., Xie, M., & Zu, Q. (2023). Electrical Automation Intelligent Control System Based on Internet of Things Technology. Electrica, 23(2).

[13] Fan, S. (2021). Electrical control online monitoring system based on internet of things. Wireless Communications and Mobile Computing, 2021(1), 2156529.

[14] Bello, O., & Zeadally, S. (2019). Toward efficient smartification of the Internet of Things (IoT) services. Future Generation Computer Systems, 92, 663-673.

[15] Hasan, M. K., Ahmed, M. M., Pandey, B., Gohel, H., Islam, S., & Khalid, I. F. (2021). Internet of Things-Based Smart Electricity Monitoring and Control System Using Usage Data. Wireless Communications and Mobile Computing, 2021(1), 6544649.

[16] Kapić Azra & Toroman Amel. (2023). Control of a Smart Security Object using an Arduino Platform and a GSM Controller. IOP Conference Series: Materials Science and Engineering,1298(1).

[17] Zhenxing Cheng,Liyi Li,Xun Bai & Jiaxi Liu. (2025). Adaptive 2-DOF H∞ robust voltage control for PMSG considering uncertain disturbances. International Journal of Electrical Power and Energy Systems,166,110582-110582.

[18] SeyyedAmirmohammad Mostafavi,Asaad Shemshadi,Reza Nazari & Hamid Yousefkhani. (2025). Utilization of H∞ robust and damping controllers with notch filters to reduce SSR in doubly-fed induction generator wind farms. Computers and Electrical Engineering,123(PA),110024-110024.

[19] Jianping Deng,Xin Meng & Baoping Jiang. (2024). Observer-Based Robust H∞ Control for Stochastic Markov Jump Delay Systems Through Dual Adaptive Sliding Mode Approach. Electronics,14(1),132-132.